Footnotes for Table II (*continued*)

1−x,−y,−z (distance 3); O_1: $^1/_2$+x,y,$^1/_2$−z and O_7: $^3/_2$−x,−y,z+$^1/_2$ (distance 4); O_{24}: x,1+y,1+z and O_{26}: x,1+y,z (distance 5); O_{20}: x,1+y,1+z and O_{18}: $^1/_2$−x,$^1/_2$+y,$^1/_2$+z (distance 6). [e] Distance across the 12-ring aperture between those oxygen atoms that in the initial, symmetric geometry of space group *P6/mmm* (No. 191) are generated from O_1 at 0.0000, 0.2754, 0.5000 and O_2 at 0.1659, 0.3318, 0.5000 by the following operations—O_1: x−y,−y,z and O_1: y,y−x,z (distance 1); O_2: x,y,z and O_2: x−y,−y,z (distance 2). [f] Distance across the 12-ring aperture between those oxygen atoms that in the initial, symmetric geometry of space group *P6/mmm* (No. 191) are generated from O_1 at 0.0000, 0.2815, 0.5000 and O_2 at 0.1639, 0.3278, 0.5000 by the following operations—O_1: x,y,z and O_1: y,y−x,z (distance 1); O_2: x,y,z and O_2: x−y,−y,z (distance 2). [g] Distance across the 12-ring aperture between those oxygen atoms that in the initial, symmetric geometry of space group $P4_122$ (No. 91) are generated from O_{31} at 0.8354, 0.8390, 0.0607 and O_{40} at 0.8356, 0.4949, 0.0608, O_{50} at 1.000, 0.8215, 0.000 and O_{60} at 1.000, 0.5126, 0.0000 by the following operations—O_{31}: x,1−y,$^1/_2$−z and O_{40}: x,y,z (distance 1); O_{60}: 1−y,x,$^1/_4$+z and O_{50}: 2−y,x,$^1/_4$+z (distance 2); O_{40}: 2−x,y,1−z and O_{31}: 2−x,1−y,$^1/_2$+z (distance 3); O_{50}: y,x,$^3/_4$−z and O_{60}: 1+y,x,$^3/_4$+z (distance 4); O_{31}: 2−y,x,$^1/_4$+z and O_{40}: 1−y,x,$^1/_4$+z (distance 7); O_{31}: x,2−y,$^1/_2$−z and O_{40}: x,1−y,$^1/_2$−z (distance 8).

with substantially increased density at the $x = \pm a$ turning points. As an example of the significance of the classical–quantum distinction we examine the Debye–Waller factor in each case. In X-ray scattering the Debye–Waller factor accounts for the effect on the scattered intensity of the density distribution of the scattering centers in direct space which is equivalent to a set of delta functions convolved with individual density functions. The scattered wave function is the Fourier transform of the scattering density, with the Debye–Waller factor arising from the convolution theorem. For a quantum harmonic oscillator, the Fourier transform of the real space Gaussian is a Gaussian in reciprocal space, as actually implemented in quantitative diffraction calculations. The Fourier transform of the classical result, eq 7, however, is a zeroeth-order Bessel function of the first kind.[53] In the present case, the atom position densities are found not to be endpoint-heavy. Apparently the multibody, statistical effects that come into play between atoms separated across the zeolite pores (5–12 Å) render classical mechanics an acceptable approximation in the present case.

(53) Weast, R. C. *CRC Handbook of Chemistry and Physics*, 68th ed.; CRC Press: Boca Raton, FL, 1987; p A-83.

Conclusion

Constant volume crystal dynamics simulations of the six representative zeolite structure types SOD (sodalite; 6-ring), RHO (rho; 8-ring), TON (theta-1; 10-ring), MFI (silicalite; 10-ring), LTL (Linde type L; 12-ring), and *BEA (beta; 12-ring) reveal substantial motion of the framework atoms about their equilibrium positions. The framework flexibilities are explicitly modeled by a crystal mechanics force field with parameters taken from quantitative interpretations of Raman and infrared spectroscopic data. The mean squared atomic displacements are, as expected, substantially smaller than the upper limit afforded by diffraction results. The increased fluctuations in the effective aperture sizes with temperature depend on the framework connectivity, also consistent with experimental observation. The frequency spectra of the O–O distances across the apertures reveal that motions of the corresponding tetrahedra are coupled. The definition, extent, and period of the fluctuations depend on the framework connectivity. It is most pronounced in the SOD and RHO frameworks, previously known from experiment to be the most susceptible to static framework distortion. The change with time in cross-sectional area of the 12-ring window in the LTL framework is cyclical, at a frequency of ~200 cm^{-1}, a clear and direct demonstration of breathing motion of the zeolite pores.

Electronic Structure and Reactivity of Dioxirane and Carbonyl Oxide

Robert D. Bach,*,[†] José L. Andrés,[†] Amy L. Owensby,[†] H. Bernhard Schlegel,[†] and Joseph J. W. McDouall[‡]

Contribution from the Departments of Chemistry, Wayne State University, Detroit, Michigan 48202, and University of Manchester, Manchester M13 9PL, United Kingdom.
Received October 28, 1991

Abstract: Dioxirane, the diradical dioxymethane, and carbonyl oxide have been studied at a variety of levels including MP2, MP4, CASSCF, QCISD, and QCISD(T). MP2 optimization is sufficient for dioxirane, the various dioxymethane biradicals, and substituted carbonyl oxide, but optimization at the QCISD or QCISD(T) level is needed to obtain the correct structure for carbonyl oxide. Significantly, both levels of theory give essentially the same C–O/O–O bond length ratio for this controversial molecule (1.281/1.369 Å and 1.287/1.356 Å for QCISD/6-31G* and QCISD(T)/6-31G**, respectively). The unsubstituted carbonyl oxide is probably anomalously sensitive to the level of calculation, since MP2/6-31G* calculations on dimethylcarbonyl oxide afford a C–O/O–O bond ratio of 1.283/1.345 Å, consistent with the higher level calculations on the parent carbonyl oxide. Transition structures have been obtained at the MP2/6-31G* level for the isomerization of carbonyl oxide to dioxirane and for the donation of oxygen from carbonyl oxide and dioxirane to ethylene. A scan of the potential energy curves for O–O bond dissociation in hydrogen peroxide and water oxide shows that the MP4SDTQ and QCISD(T) curves are nearly superimposable for bond elongation up to 2.5 Å. At the QCISD(T)/6-31G*//MP2/6-31G* level, carbonyl oxide is 28.6 kcal/mol higher than dioxirane and separated from it by a barrier of 19.1 kcal/mol; the barriers for donation of an oxygen atom from dioxirane and carbonyl oxide to ethylene are 16.7 and 11.9 kcal/mol, respectively. The MP4SDTQ level is adequate for determining the barriers for the first two reactions, but QCISD(T) is required for a proper treatment of the barrier for dioxirane plus ethylene (MP4 overestimates the triples contribution). Theoretical evidence is presented that suggests that both the reactants and the transition structures involved in these epoxidation reactions are principally closed shell in nature.

Introduction

Although a dioxirane has only recently been isolated and characterized by Murray,[1a] earlier experimental work by Edwards and Curci[1b] stimulated the theoretical community[2] to calculate the chemical and physical properties of the parent dioxirane (**1**)

[†] Wayne State University.
[‡] University of Manchester.

(1) (a) Murray, R. W.; Jeyaraman, R. *J. Org. Chem.* **1985**, *50*, 2847. (b) Curci, R.; Fiorentino, M.; Troisi, L.; Edwards, J. O.; Pater, R. H. *J. Org. Chem.* **1980**, *45*, 4758. (c) Bunnelle, W. H. *Chem. Rev.* **1991**, *91*, 335.

0002-7863/92/1514-7207$03.00/0

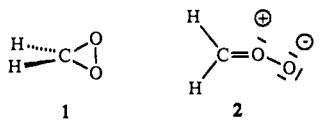

1 2

and its more elusive tautomer, carbonyl oxide (**2**).[1c] In the relatively short history[3] of this class of oxidant, dimethyldioxirane[4] and several related peroxo species[4c] have proven to be powerful oxygen atom transfer reagents of unusual synthetic utility. It is now well established that dioxirane (**1**) is more stable than its dioxygen ylide (**2**) and that the respective barriers for their interconversion are sufficiently high that each exhibits its own chemical behavior when independently generated. Calculated[2] energy differences between these isomeric peroxy compounds range from 29.7 to 54.1 kcal/mol, while the theoretical estimates of the barrier for ring closure of **2** to **1** range from 20 to 33.6 kcal/mol.[2a,3b] The electronic structure and chemical reactivity of these isomeric peroxo compounds have been the subject of considerable controversy for many years. While **1** has mainly served as a novel oxygen donor, carbonyl oxides can also undergo cycloaddition reactions. A second point of major concern is whether carbonyl oxide is best described as a zwitterionic species as depicted in **2** or as a biradical. On the basis of a mechanistic study involving competitive oxidation of sulfides and sulfoxides, Adam[4a] has suggested that the highly strained cyclic peroxo functionality is less nucleophilic than the higher energy open carbonyl oxide structure. However, Baumstark[4b] has cautioned that a clear distinction between nucleophilicity and electrophilicity may be more elusive than initially anticipated. In a preliminary report, we suggested that the intrinsic gas-phase reactivity of these two oxygen donors is the opposite of the reactivity found in solution.[7d]

We now provide additional data concerning the level of theory essential to the accurate prediction of transition-state structures and energies for the epoxidation of ethylene by these unique oxygen atom donors.

Method of Calculation

Molecular orbital calculations were carried out using the GAUSSIAN 90 program system[5] utilizing gradient geometry optimization.[5b] The structures for dioxirane (**1**), carbonyl oxide (**2**), the transition state between **1** and **2** (**TS-2**), and the transition states for oxygen transfer from **1** and **2** to ethylene (**TS-3** and **TS-4**) have been optimized with the 3-21G and 6-31G* basis sets by both Hartree–Fock (HF) and second-order Møller–Plesset perturbation theory (MP2); reoptimization using the quadratic configuration interaction approach[5c] (QCISD, full) with the 3-21G basis set and comparison with the MP2/3-21G structures indicate that the effects of higher levels of electron correlation are not important for the geometries of these transition states. Final geometry optimizations were carried out by MP2 theory with the 6-31G* basis set (i.e. MP2/6-31G*); this level of theory has already been shown to be reliable for these systems.[2a,7] Relative energies and barrier heights were computed with the 6-31G* basis set using spin-restricted second-, third-, and fourth-order Møller–Plesset perturbation theory[5d] (MP2/6-31G*, MP3/6-31G*, and MP4SDTQ/6-31G*, respectively; frozen core) and using quadratic configuration interaction with perturbative corrections for triple excitations (QCISD(T)/6-31G*, frozen core). The notation QCISD(T)/6-31G*//MP2/6-31G* is used to indicate a QCISD(T) single-point calculation with the 6-31G* basis set using the geometry optimized at the MP2 level with the 6-31G* basis set. Note that all the post-SCF optimizations are carried out including all the MO's in the electron correlation calculation and that the single-point post-SCF energies are computed with the frozen-core approximation. The QCISD(T)/6-31G*//MP2/6-31G* level is sufficiently accurate to allow considerable confidence in the relative barrier heights. To answer some of the questions about the significance of electron transfer and biradical character in the transition states, a series of complete active-space multiconfigurational SCF (CASSCF) calculations were carried out using geometries optimized by configuration interaction with single and double excitations (CISD, full) and the 3-21G basis set. The geometries of **TS-3**, **TS-4**, and **TS-5** were constrained to a symmetrical spiro orientation. A full set of vibrational frequencies were calculated for transition structures **TS-2**, **TS-3**, and **TS-4** at the HF/6-31G* level and for **TS-5** at HF/3-21G using analytical second derivatives, and only one imaginary frequency was found for each TS. The transition structures **TS-2**, **TS-3**, and **TS-4** were established to be stationary points at the MP2/6-31G* level, and TS-5 was established to be a stationary point at the HF/6-31G* level. Frequency calculations at the MP2/6-31G* level established **TS-3a** and **TS-4a** to be first-order transition states having only one imaginary frequency. However, **TS-3** and **TS-4** are second-order saddle points at this level of theory.

Results and Discussion

Electron Correlation in the O–O Bond. The ground-state scission of the oxygen–oxygen bond is involved in a great many condensed-phase chemi- and bioluminescence reactions.[6a,b] Historically, it has been perceived that calculational requirements for energy surfaces involving the O–O bond are often beyond the limits of available code. Cleavage of the peroxide bond is of the $(\sigma\pi)(\sigma\pi)$ type, resulting in four pairs of biradical states.[6c] Clearly, one would prefer a balanced treatment of both dynamic and static electron correlation effects, but on the larger, more chemically interesting systems that we prefer to study, treatment of these combined effects is not yet feasible. We have pointed out that dynamic correlation at the MP2 level of theory is adequate for geometries,[7] and limited CASSCF calculations on selected oxygen-transfer reactions from water oxide have suggested that static correlation corrections are not that important in the cleavage of a dipolar O–O bond.[7c]

In our earlier studies[7b,c] on the O–O bond, we addressed potential problems concerning the E_{4T} triples contribution to the correlation energy for rearrangement of H_2O_2 to water oxide[8] (H_2O^+–O^-) calculated with the 6-31G* basis set. We found that both geometry and energy had to be calculated at a correlated level of theory (MP4SDTQ/6-31G*//MP2/6-31G*) in order to

(2) (a) Cremer, D.; Schmidt, T.; Gauss, J.; Radhakrishnan, T. P. *Angew. Chem., Int. Ed. Engl.* **1988**, *27*, 427. (b) Cremer, D.; Schindler, M. *Chem. Phys. Lett.* **1987**, *133*, 293. (c) Gauss, J.; Cremer, D. *Chem. Phys. Lett.* **1989**, *163*, 549; **1987**, *133*, 420. (d) Karlström, G.; Engström, S.; Jönsson, B. *Chem. Phys. Lett.* **1979**, *67*, 343. (e) Karlström, G.; Roos, B. O. *Chem. Phys. Lett.* **1981**, *79*, 416. (f) Sawaki, Y.; Kato, H.; Ogata, Y. *J. Am. Chem. Soc.* **1981**, *103*, 3832. (g) Harding, L. B.; Goddard, W. A., III *J. Am. Chem. Soc.* **1978**, *100*, 7180. (h) Wadt, W. R.; Goddard, W. A., III *J. Am. Chem. Soc.* **1975**, *97*, 3004. (i) Ha, T.-K.; Kühne, H.; Vaccani, S.; Günthard, H. H. *Chem. Phys. Lett.* **1974**, *24*, 172. (j) Cremer, D.; Bock, C. W. *J. Am. Chem. Soc.* **1986**, *108*, 3375. (k) Replogle, E. S.; Pople, J. A. *Abstracts of Papers*, 202nd National Meeting of the American Chemical Society, New York, 1991; American Chemical Society: Washington, DC, 1991. (l) Rahman, M.; McKee, M. L.; Shevlin, P. B.; Sztyrbicka, R. *J. Am. Chem. Soc.* **1988**, *110*, 4002.

(3) (a) Adam, W.; Curci, R.; Edwards, J. O. *Acc. Chem. Res.* **1989**, *22*, 205. (b) Murray, R. W. *Chem. Rev.* **1989**, *89*, 1187. (c) Curci, R. *Advances in Oxygenated Processes*; Baumstark, A. L., Ed.; JAI Press: Greenwich, CT, 1990; Vol. 2, Chapter 1, pp 1–59.

(4) (a) Adam, W.; Chan, Y.-Y.; Cremer, D.; Gauss, J.; Scheutzow, D.; Schindler, M. *J. Org. Chem.* **1987**, *52*, 2800. Adam, W.; Haas, W.; Lohray, B. B. *J. Am. Chem. Soc.* **1991**, *113*, 6202. (b) Baumstark, A. L.; Vasquez, P. C. *J. Org. Chem.* **1988**, *53*, 3437. (c) Mello, R.; Fiorentino, M.; Sciacovelli, O.; Curci, R. *J. Org. Chem.* **1988**, *53*, 3891. (d) Murray, R. W.; Shiang, D. L.; Sinsh, M. *J. Org. Chem.* **1991**, *56*, 3677. (e) Adam, W.; Haas, W.; Sieker, F. *J. Am. Chem. Soc.* **1984**, *106*, 5020.

(5) (a) Frisch, M. J.; Head-Gordon, M.; Trucks, G. W.; Foresman, J. B.; Schlegel, H. B.; Raghavachari, K.; Robb, M. A.; Binkley, J. S.; Gonzalez, C.; Defrees, D. J.; Fox, D. J.; Whiteside, R. A.; Seeger, R.; Melius, C. F.; Baker, J.; Martin, R. L.; Kahn, L. R.; Stewart, J. J. P.; Topiol, S.; Pople, J. A. *GAUSSIAN 90*; Gaussian Inc.: Pittsburgh, PA, 1990. (b) Schlegel, H. B. *J. Comput. Chem.* **1982**, *3*, 214. (c) Pople, J. A.; Head-Gordon, M.; Raghavachari, K. *J. Chem. Phys.* **1987**, *87*, 5968. (d) Møller, C.; Plesset, M. S. *Phys. Rev.* **1934**, *46*, 618. For a review of coupled cluster and many-body perturbation methods see: Bartlett, R. J. *Annu. Rev. Phys. Chem.* **1981**, *32*, 359. (e) Bofill, J. M.; Pulay, P. *J. Chem. Phys.* **1989**, *90*, 3637.

(6) (a) Turro, N. J.; Nechtken, P.; Schore, N. E.; Schuster, G.; Steinmetzer, H. C.; Yekta, A. *Acc. Chem. Res.* **1974**, *7*, 97. (b) Adams, W. *J. Chem. Educ.* **1975**, *52*, 138. (c) Dauben, W. G.; Salem, L.; Turro, N. J. *Acc. Chem. Res.* **1975**, *8*, 41.

(7) (a) Bach, R. D.; McDouall, J. J. W.; Owensby, A. L.; Schlegel, H. B. *J. Am. Chem. Soc.* **1990**, *112*, 7064. (b) Bach, R. D.; McDouall, J. J. W.; Owensby, A. L.; Schlegel, H. B. *J. Am. Chem. Soc.* **1990**, *112*, 7065. (c) Bach, R. D.; Owensby, A. L.; González, C.; Schlegel, H. B.; McDouall, J. J. W. *J. Am. Chem. Soc.* **1991**, *113*, 6001. (d) Bach, R. D.; Owensby, A. L.; Andrés, J. L.; Schlegel, H. B. *J. Am. Chem. Soc.* **1991**, *113*, 7031. (e) Bach, R. D.; Owensby, A. L.; González, C.; Schlegel, H. B. *J. Am. Chem. Soc.* **1991**, *113*, 2338. (f) Bach, R. D.; Coddens, B. A.; McDouall, J. J. W.; Schlegel, H. B.; Davis, F. A. *J. Org. Chem.* **1990**, *55*, 3325. (g) Bach, R. D.; Andrés, J. L.; Davis, F. A. *J. Org. Chem.* **1992**, *57*, 613.

(8) Pople, J. A.; Raghavachari, K.; Frisch, M. J.; Binkley, J. S.; Schleyer, P. v. R. *J. Am. Chem. Soc.* **1983**, *105*, 6381.

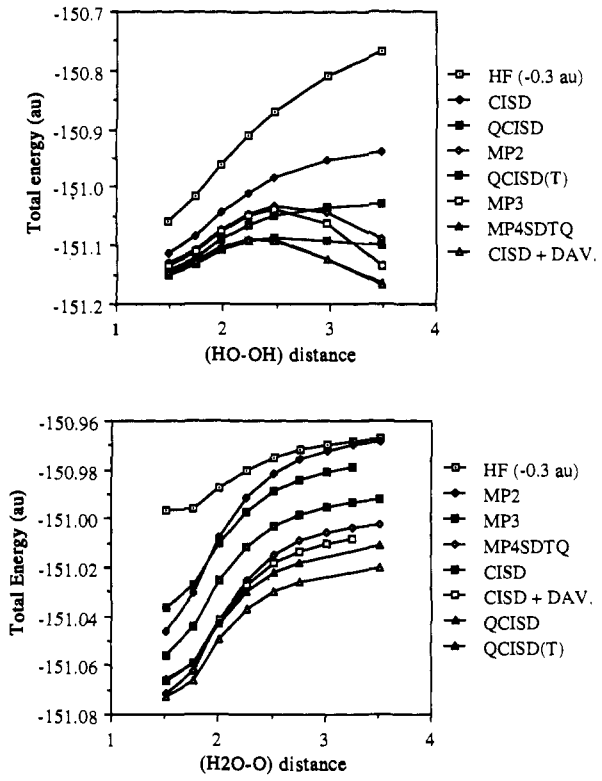

Figure 1. Potential energy curves for O–O bond dissociation (6-31G*) in (a, top) hydrogen peroxide and (b, bottom) water oxide (HF energies offset by 0.3 au to put them on the same scale as the correlated energies).

find a barrier (3.9 kcal/mol with ΔZPE) for reversion of water oxide to H_2O_2 (eq 1).[7c] Geometry optimization at the

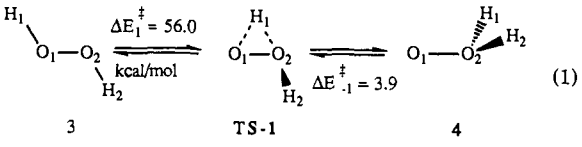

(1)

MP4SDTQ/6-31G* level resulted in a barrier difference of only 0.2 kcal/mol and a change in O–O bond distance at the TS of 0.057 Å. The O–O bond in the TS for oxygen transfer from water oxide to ammonia was also 0.042 Å longer at the QCISD than at the MP2 level (6-31G*), and both activation barriers were in excellent agreement.

In a preliminary account of calculations on the barriers for oxygen transfer from dioxirane and carbonyl oxide to ethylene,[7d] we reported that the inclusion of triples at the QCI level was essential to describe adequately the energy of the strained O–O bond in dioxirane. In related oxygen-transfer reactions, we have noted O–O bond lengths in transition-state structures approaching ~2.0 Å. Because of the historical difficulty attending the dissociation of the O–O bond, we thought it prudent to examine the potential energy curve for O–O bond rupture in both types of O–O bonds (HO–OH and H_2O^+–O^-) that we are studying using the various levels of theory that we are employing with particular emphasis on the effects of electron correlation correction.

In Figure 1a, a scan of the energy as a function of O–O bond length for H_2O_2 (**3**) clearly shows the effect of the triples contribution. The calculated energies for fourth-order Møller–Plesset perturbation theory (MP4SDTQ), quadratic configuration interaction with triples (QCISD(T)), and conventional configuration interaction including the Davidson correction (CISD+Dav) are all essentially superimposed at O–O bond distances up to 2.5 Å. As the O–O bond stretches toward dissociation, the convergence of the Møller–Plesset series becomes sufficiently poor that the MP2, MP3, and MP4 surfaces are highly distorted and the corresponding energies fall below the dissociation limit. The

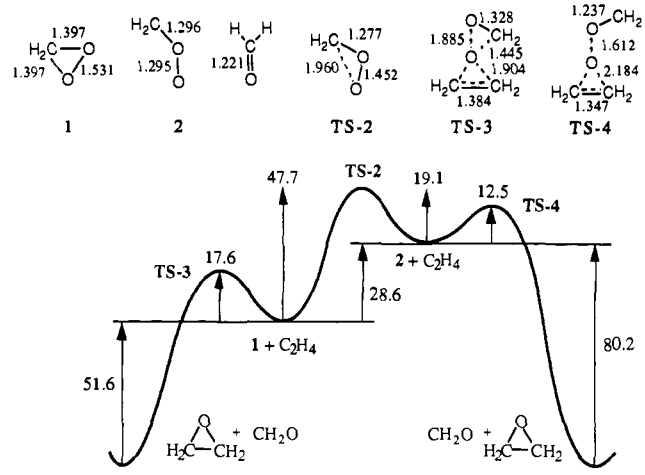

Figure 2. Potential energy diagram for the interconversion of dioxirane and carbonyl oxide and for oxygen atom transfer to ethylene. Geometries are at MP2/6-31G* and energies (kcal/mol) are at RQCISD(T)/6-31G*//MP2/6-31G*.

QCISD(T) surfaces do not suffer from this problem. However, as Figure 1a shows, the problem with the MP_n surfaces does not manifest itself until the O–O bond has stretched beyond ~2.5 Å. For example, if we calculate the energy difference between H_2O_2 at R(O–O) = 2.232 Å and two OH radicals at the QCISD(T)/6-31G* level, we obtain 11.4 kcal/mol. A similar calculation at the MP4SDTQ/6-31G* level yields 10.4 kcal/mol, indicating that the MP4SDTQ level of theory is capable of estimating the energetics of the O–O bond at these geometries. The comparable potential energy curves for water oxide (**4**), shown in Figure 1b, also indicate that the MP_n surfaces are well-behaved at distances up to 2.5 Å for this system. When the geometry of the water fragment is fully optimized (MP2/6-31G*) at two selected points of O–O bond elongation (2.267 and 3.517 Å), the total energies differ from that of isolated $H_2O + {}^1O$ by 11.0 and 0.95 kcal/mol at QCISD(T)/6-31G* and by 16.4 and 1.4 kcal/mol at MP4SDTQ/6-31G*, respectively. Since the O–O bond lengths in transition structures that we have studied to date are typically less than 2.2 Å, these data support our earlier contention[7] that calculations at the MP4SDTQ/6-31G*//MP2/6-31G* level afford geometries and energies sufficiently reliable for the study of oxygen atom transfer from a peroxide. In his exemplary studies on the dioxirane–carbonyl oxide rearrangement, Cremer has also stressed the importance of carrying out studies at the MP2/6-31G* level of theory with MP4SDTQ correlation corrections to the energy.[2a] However, with molecules like carbonyl oxide, where a high degree of biradical character has been suggested,[2g,h] the triples contribution must be given careful consideration as discussed below.[2c]

Dioxirane and Isomeric Biradicals. Since the ground state of these highly reactive oxygen atom donors can potentially be described as biradicals, the possibility of contributions from excited electronic configurations is more prevalent than usual. The weakest bond in the dioxirane molecule is the peroxide bond that has an estimated O–O bond dissociation energy (BDE) of ~36 kcal/mol.[2a] A fundamental question that we wish to address is the extent of the electron population in the σ^*(O–O) bond and its contribution to the inherent reactivity of this highly strained oxygen donor. These concerns are particularly relevant in the context of a generalized valence bond (GVB) study on both dioxirane and carbonyl oxide. In this seminal study by Goddard[2g,h] using a DZP basis, it was suggested that the biradical form, dioxymethane (OCH_2O), resulting from homolytic O–O bond rupture could make a contribution to the chemistry of the parent dioxirane. Bond distances of 1.45 Å for the cyclic peroxide **1** and 2.25 Å for this bis(oxy)methylene biradical were assumed for the O–O bond in these two isomers. The ground state of dioxymethane was found to be a singlet biradical ($^1A_1$) that has both π-type atomic p orbitals on oxygen singly occupied with the two oxygen

lone pairs in the plane of the ring (**5a**). Adhering to the Goddard

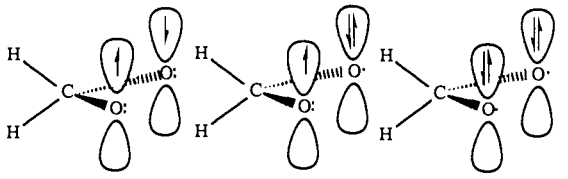

5a (2π) 5b (3π) 5c (4π)

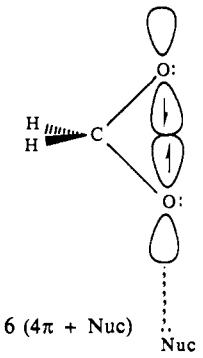

6 (4π + Nuc)

nomenclature, this structure is referred to as the "2π configuration" and the 2s electrons are omitted for clarity. The singlet 4π state (**5c**) with the two π orbitals doubly occupied was calculated to be 11.3 kcal/mol higher in energy. A 3π state (**5b**) was intermediate in energy, being 8.9 kcal/mol above that of the 2π biradical (**5a**). Significantly, at this level of theory (GVB(3)-CI), the lowest biradical **5a** was found to be only 11.1 kcal/mol above the ground state of the cyclic peroxide, dioxirane (**1**). By combining this value with higher level (GVB(7/17)-CI) calculations on the 4π radical and empirical corrections to the BDE's, Goddard et al. estimated that **5a** lies approximately 15 kcal/mol above dioxirane. The inherent difficulty in an adequate theoretical treatment of dioxirane can clearly be traced to these low-lying excited states. Table I catalogues an investigation into the relative stabilities of the isomeric forms.

Since we calculated an O–O bond distance in the transition structure (**TS-3**) of 1.885 Å for oxygen donation from dioxirane to ethylene, a comparable O–O bond distance (2.25 Å) in the biradical suggests it could be implicated in oxygen transfer. However, oxygen atom transfer from dioxirane involves an S_N2-like displacement along the O–O bond axis with concomitant breaking of the σ(O–O) bond. Such a TS correlates with the 4π configuration affording the ground state of formaldehyde as shown in **6**. This presents an interesting enigma because any biradical character in the TS for oxygen transfer where the O–O σ bond is being broken must involve the 4π biradical that lies 26.4 kcal/mol above the open-shell 2π system and is 38.0 kcal/mol higher in energy than ground-state dioxirane at the QCISD-(T)/6-31G* level. Although the 4π biradical can be stabilized at the TS geometry, extensive involvement of an open-shell pathway for O–O bond cleavage as depicted in **6** would obviously exact a high energetic price.

Since ab initio SCF analysis with second-order Møller–Plesset perturbation theory is not capable of describing ozone,[2e] similar computational difficulties should also be anticipated for carbonyl oxide. The GVB analysis of carbonyl oxide (peroxymethylene) suggests that the gas-phase ground state is the planar singlet 1,3-biradical **7a** ($^1A'$, 4π) which bears a similarity to ozone.[2g,h] The lowest vertical excited state of peroxymethylene is 1.2 eV (27.7 kcal/mol) above the singlet and results from triplet coupling of the terminal π orbitals. Oxygen transfer from carbonyl oxide also involves a symmetry crossing problem that is almost the antithesis of that noted above for dioxirane. Neither **7a** nor the higher lying (1.7 eV) singlet biradical **7b**, with the terminal oxygen doubly occupied (5π, $^1A''$ state), correlates with the product, formaldehyde, resulting from singlet oxygen atom transfer. Oxygen transfer by a direct S_N2 displacement on the terminal oxygen

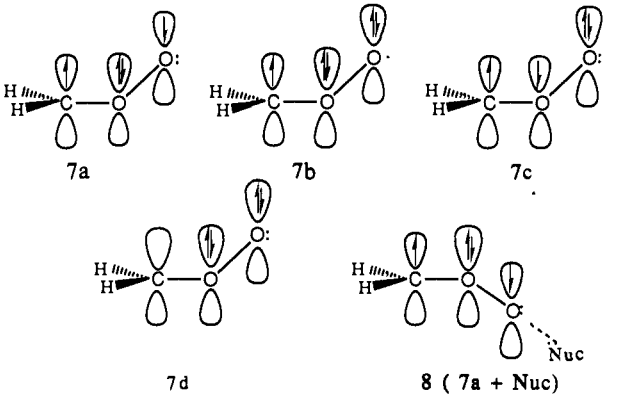

7a 7b 7c

7d 8 (7a + Nuc)

involving these discrete electronic states would afford formaldehyde in its $n \rightarrow \pi^*$ excited state as shown in **8**. Promotion of an electron from the central to the terminal oxygen affords zwitterionic structure **7c**, which is 3.99 eV higher in energy than ground state **7a** on the basis of a calculated vertical excitation energy (GVB-CI).[2g] This higher energy configuration **7c** would be required in order to effect oxygen transfer, producing the ground state of the carbonyl moiety. This structure is of course carbonyl oxide with a complete octet of electrons (including 2s) around the "electrophilic" oxygen. This analysis again suggests that the electronic configuration of the TS should be largely closed shell in nature, but the energetic requirements for this closed-shell configuration would appear to be prohibitive if indeed singlet 1,3-biradical **7a** represents the ground state of carbonyl oxide.

Having introduced both state-function correlation problems associated with reactants **1** and **2**, we examined the magnitude of open-shell involvement in oxygen atom transfer next. The description of dioxirane poses certain difficulties for the Hartree–Fock model. The closed-shell description shows a RHF → UHF instability, indicating that the wave function does not have sufficient flexibility to describe this molecule correctly. The alternative approach is to use UHF theory, but this suffers from the lack of correct spin symmetry. Multireference schemes such as the CASSCF method are capable of overcoming the inadequacies of Hartree–Fock models by providing a general treatment of the internal correlation problem. However, the main weakness of the multiconfigurational schemes is the difficulty involved in treating the dynamic correlation. Single-reference methods which include subsets of excitations to infinite order by using a cluster expansion of the wave function have been shown to yield accurate energies and geometries for species with biradical character.[2c,k] While these methods solve many of the problems mentioned above, they are less satisfying from a "modeling" point of view, since the various contributions to the correlation problem are intertwined in a high-order wave function which is difficult to interpret in terms of the concepts familiar from qualitative discussions of electronic structure. In order to retain some connection with simple orbital concepts, while maintaining a high level of quantitative accuracy, we have chosen to pursue the problem at hand from a variety of computational perspectives.

Goddard's earlier investigation into the nature of the open biradical forms of dioxirane employed GVB wave functions with the perfect-pairing/strong-orthogonality restriction.[2g] The CASSCF description of these structures is capable, with a suitable choice of active space, of describing the ground state of the open form with no preconceptions regarding the orientation of the radical. In the CASSCF representation, the 2π, 3π, and 4π singlet biradicals described by Goddard will manifest themselves as different roots of the multiconfigurational secular problem, with the orbitals being optimal for the lowest root. To this end, the simplest active space we can choose for comparison with Goddard's work will consist of the two σ orbitals describing the O–O bond and the two π orbitals (bonding and antibonding) lying perpendicular to the σ orbitals. Into this space we then distribute the six electrons which come from the two oxygen lone pairs and the σ(O–O) bond in all possible ways. This yields a modest calculation

Table I. Geometries (Å) and Energies (au) for Dioxirane and Dioxymethane

		dioxymethane biradicals		
	dioxirane (**1**)	2π (**5a**)	3π (**5b**)	4π (**5c**)
		UHF/3-21G		
energy	−187.554 94[a]	−187.624 794[a]	−187.610 485[b]	−187.594 353[b]
$\langle S^2 \rangle$	0.23	1.01	1.01	1.00
R(O–O)	1.52	2.40		
R(C–O)	1.43	1.41		
nat orb occ				
σ(O–O)	1.88	2.00	1.97	1.00
σ^*(O–O)	0.12	2.00	1.00	1.00
π(O–O)	2.00	0.94	1.00	2.00
π^*(O–O)	2.00	1.06	2.00	2.00
		CAS (2,2)/6-31G*		
energy	−188.600 49[a]	−188.657 44[a]		
R(O–O)	1.618	2.326		
R(C–O)	1.363	1.359		
nat orb occ				
σ(O–O)	1.84	2.00		
σ^*(O–O)	0.16	2.00		
π(O–O)	2.00	0.80		
π^*(O–O)	2.00	1.20		
		MP2/6-31G*		
energy	−189.107 819[a,c]	−189.070 617[a]	−189.060 069[a]	−188.977 685[a]
$\langle S^2 \rangle$		1.01	1.05	1.07
R(O–O)	1.530	2.350	2.138	2.203
R(C–O)	1.398	1.367	1.352	1.367
		CISD/6-31G*		
energy	−189.063 996[a,c]			
R(O–O)	1.489			
R(C–O)	1.380			
		QCISD/6-31G*		
energy	−189.120 919[a,c]	−189.084 601[a,c]		
R(O–O)	1.522	2.363		
R(C–O)	1.393	1.306		
		PMP2/6-31G*//MP2/6-31G*		
energy[d]	−189.098 067	−189.068 180	−189.050 061	−188.925 292
ΔE (kcal mol^{-1})	0.0	18.8	30.1	108.4
		PMP4/6-31G*//MP2/6-31G*		
energy[d]	−189.129 663	−189.111 825	−189.089 022	−188.976 997
ΔE (kcal mol^{-1})	0.0	11.2	25.5	95.8
		QCISD(T)/6-31G*//MP2/6-31G*		
energy[d]	−189.128 088	−189.109 579	−189.091 170	−189.067 477
ΔE (kcal mol^{-1})	0.0	11.6	23.2	38.0
		QCISD(T)/6-31G*//QCISD/6-31G*		
energy[d]	−189.127 959	−189.108 145		
ΔE (kcal mol^{-1})	0.0	12.4		

[a] Geometry optimized at the level indicated. [b] Energy calculated at the 2π biradical geometry. [c] Closed-shell calculation based upon an RHF reference. [d] Energies calculated with the frozen-core approximation.

which should be capable of accounting for the structure-dependent internal correlation.

A calculation on the parent dioxirane shows the CASSCF natural orbital occupation numbers to be 1.84 and 0.16 for the σ(O–O) and σ^*(O–O) orbitals respectively. The π and π^* orbitals are both doubly occupied (occupancy >1.99). Two important conclusions may be drawn from this result: (i) the instability of the RHF wave function for dioxirane[9] is clearly a result of the high occupancy of the σ^*(O–O) orbital, and (ii) the correct description of the internal correlation requires only the two electrons and orbitals of the O–O σ bond.

A similar picture emerges for the 2π configuration of the open form of dioxirane. A CASSCF calculation with the larger active space described above shows that π^* and π orbitals to have an occupancy of 1.20 and 0.80, respectively, with the σ and σ^* orbitals being doubly occupied. Our calculation agrees with Goddard's in predicting the 2π biradical form of bis(oxy)methylene to be the lowest in energy. Again, only the two π orbitals need be correlated with two electrons.

Using the more limited two-electron/two-orbital active spaces, the geometry of dioxirane and bis(oxy)methylene were optimized at the CASSCF/6-31G* level (Table I). Comparing the geometries at various levels of theory for bis(oxy)methylene shows this structure to be much less sensitive to correlation effects than dioxirane. In dioxirane, the C–O bond is not affected by the level of correlation as distinctly as the O–O bond; the latter is clearly a result of the high occupancy of the σ^*(O–O) orbital. Having addressed the electronic structure of the closed and open forms of dioxirane, we must look at the energetics of these structures. To obtain good estimates of the relative stabilities, we must take into account the dynamic electron correlation. While the energies show significant change with the level of theory, the geometries are less sensitive. Hence, all three biradical forms and the parent dioxirane were optimized at the UMP2/6-31G* level. Energies were then calculated at the second and fourth orders of perturbation theory, including spin projection according to the scheme proposed by Schlegel (PMP*n*),[10] and also at the higher quadratic

(9) The root of the RHF → UHF stability analysis was relatively small (−0.05), and release of the RHF constraint (HF/3-21G) and reoptimization of the molecular orbitals affording a UHF stable wave function resulted in a decrease in total energy of only 1.8 kcal/mol.

configuration interaction level, including a perturbative treatment of the triples correct to fourth order (QCISD(T)). As may be seen from Table I, dynamic correlation has a dramatic effect on the calculated stabilities. The most extreme problem is manifested for the 4π structure, which is the one most relevant in discussing the reactivity of dioxirane in oxygen-transfer processes. This again highlights the need to include high-order correlation in order to obtain reliable energies.

Our best calculation of the dioxirane/bis(oxy)methylene stability is 12.4 kcal/mol and is obtained from geometries optimized at the QCISD(T) level. Goddard's estimate of this stability is ca. 15 kcal/mol.[2g]

We are obliged to spend considerably less effort to bring calculations on carbonyl oxide up to state-of-the-art because of the rigorous calculations recently reported by Gauss and Cremer.[2c] Because of the flat potential energy surface for stretching the O–O bond, highly accurate calculations are required to obtain good geometry predictions. Cremer et al.[2c] have optimized the geometry of carbonyl oxide at the HF, MP2, MP4SDQ, MP4SDTQ, and QCISD(T) levels of theory using the 6-31G(d,p) basis sets. The MP2/6-31G* C–O and O–O bonds are almost identical (1.297 and 1.294 Å), implicating resonance structure **7a** as being a major

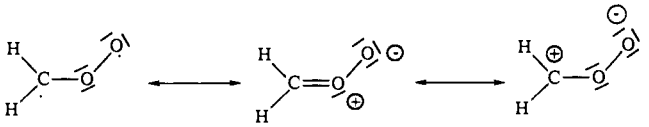

7a and 7b 7c 7d

contributor. Full geometry optimization[2c] at QCISD(T)/6-31G-(d,p) gave corresponding bond distances of 1.287 and 1.356 Å, which suggests that the electronic structure for CH_2OO is closed shell in nature and is best described by classical resonance structures **7c** and **7d**. It was suggested that the ratio of C–O/O–O bond lengths is a good approximation to its electronic structure. However, geometry optimization at the MP4 level, with triple excitation, gave C–O/O–O bond lengths of 1.314/1.306 Å. Since the QCISD(T)-optimized structure was 1.64 mhartrees below the MP4SDTQ structure despite the fact that the QCISD(T) correlation energy was 6.95 mhartrees smaller, it was concluded that the former level of theory gave the best description of CH_2OO.[2c] Partial geometry optimization in a small MCSCF calculation using ten selected configurations also predicted a shorter O–O bond length with a ratio of 1.277/1.262 Å, and a biradical structure was suggested.[2d] The largest CASSCF calculation to date,[2e] with ten electrons in eight active orbitals and 1176 configurations, afforded a single minimum with C–O and O–O bond lengths of 1.275 and 1.313 Å. The potential energy surface was found to be very flat, and the CASSCF wave function changed drastically with the O–O bond length, resulting in a change in the dipole moment from 3.8 D at the equilibrium geometry to 5.0 D at R(O–O) = 1.5 Å. This indicates that the closed-shell zwitterionic structures **7c** and **7d** become increasingly important as the O–O bond is elongated. From this it was also concluded that carbonyl oxides should be extremely sensitive to solvent effects.

The pervasive contention that one must account for the contribution of triple substitutions to both the energy and geometry when the potential for a biradical species exists is further clouded by our observation that the QCISD/6-31G* optimization of CH_2OO (i.e. without triples) gave C–O and O–O bond distances of 1.281 and 1.369 Å in good accord with the QCISD(T)/6-31G(d,p) geometry (1.287 and 1.356 Å). This calculated geometry is not altered by the more flexible 6-31G** basis set, since we observe an identical bond ratio. Thus, the change in bond lengths as a function of the level of theory is not necessarily a matter of needing the triples contribution, but rather a problem with the MP4 overestimation of the effect of the singles and triples. The QCI calculations predict an O–O bond length that is 0.04–0.05 Å longer than that found in the extensive CASSCF calculation.[2c]

(10) (a) Schlegel, H. B. *J. Phys. Chem.* **1988**, *92*, 3075. (b) Schlegel, H. B. *J. Chem. Phys.* **1986**, *84*, 4530.

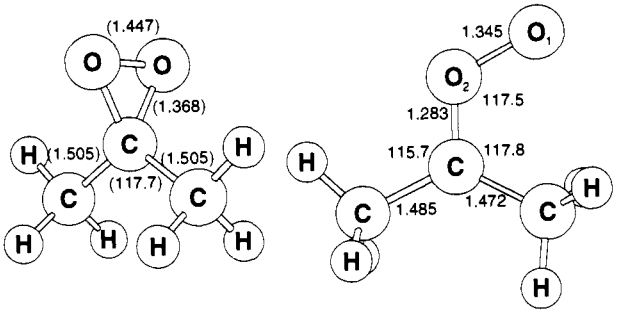

Figure 3. Geometries of dimethyldioxirane and dimethylcarbonyl oxide at MP2/6-31G* (HF/6-31G* values in parentheses). Distances are in angstroms, and angles in degrees. Energies: (−266.699 55), −267.423 89 au.

The important point is that both QCI and CASSCF methods of calculation afford an electronic structure for the parent carbonyl oxide that supports a closed-shell structure.

On the basis of our prior experience, we were not surprised to find that the QCISD/6-31G*-optimized structure of CH_2OO had a HF wave function that was RHF → UHF unstable with a root = −0.058. Removal of the RHF constraint and reoptimization of the MO's gave an energy that was 8.6 kcal/mol lower. Computation of the total energy with the triples contribution showed that the QCISD(T) closed-shell wave function was 7.1 kcal/mol *lower* in energy than the QCISD(T) open-shell wave function. The HOMO–LUMO natural orbital occupations for the UHF wave function are 1.34 and 0.66 electrons. However, the LUMO orbital occupation was markedly reduced even by a very limited CAS (2,2)/6-31G* calculation (at the QCISD geometry) that predicted orbital occupations of 1.89 and 0.11 electrons with CI coefficients of −0.9712 and 0.2382. This analysis also suggests that CH_2OO is largely (~94%) a closed-shell species best described by resonance structures **7c** and **7d**.

Introduction of alkyl groups also affects the fundamental structure of the parent carbonyl oxide by mixing filled methyl group orbitals with π-symmetry (π-CH_2) with the "allylic" C–O–O π-system of carbonyl oxide. The C–O and O–O bond distances for dimethylcarbonyl oxide at the MP2/6-31G* level of 1.283 and 1.345 Å, respectively (Figure 3), are consistent with resonance structures **7c** and **7d** and the QCI-optimized structure of the unsubstituted carbonyl oxide. Attack of closed-shell nucleophiles (NH_3, CH_2CH_2) on the terminal oxygen of **2** also affords a closed-shell transition structure as seen in **TS-3** and **TS-4**. We suggest that the MP2 level of theory is adequate to describe the geometry of the transition structures for oxygen atom transfer from both dioxirane and carbonyl oxide. In the comparison of theoretical and experimental results, one must always keep in mind the fact that the parent carbonyl oxide may indeed have a different electronic structure than the disubstituted oxygen donors used in the laboratory. Substituents may well have a more profound effect upon the electronic structure of the functional group itself than other aspects of chemical reactivity. Although the zwitterionic structure **2** has a formal positive charge on O_2, the Mulliken charges on O_1 and O_2 are −0.44 and −0.10, respectively. The calculated charges on O_1 and O_2 for dimethylcarbonyl oxide are −0.48 and −0.24.

Rearrangement of Dioxirane to Carbonyl Oxide. Karlström and Roos have also done an extensive MCSCF calculation on the transition structure of the rearrangement of carbonyl oxide to dioxirane.[2e] They obtained an O–O bond distance of 1.524 Å (Table IIa) and reported a barrier of 23.9 kcal/mol at the MR-CI level with second-order perturbation theory for the dynamical correlation. They found orbital occupancies of greater than 1.85 for all pertinent orbitals, suggesting that this is largely a closed-shell transition structure. We calculated an MP4SDTQ/6-31G*//MP2/6-31G* barrier of 23.8 kcal/mol. This barrier (Table IIIb) was reduced to 19.1 kcal/mol (Figure 3) at the comparable QCISD(T) level, again pointing out the overestimation of the triples contribution in the MP4 formalism.

Table II[a]

a. Optimized Geometries for Dioxirane to Carbonyl Oxide Rearrangement

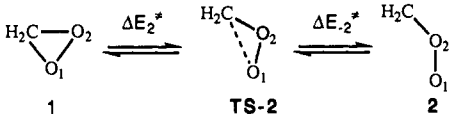

1 **TS-2** **2**

Dioxirane (**1**)

	HF/3-21G	MP2/3-21G	QCISD/3-21G	HF/6-31G*	MP2/6-31G*
$R(CO_1)$	1.428	1.481	1.475	1.358	1.397
$R(CO_2)$	1.428	1.481	1.475	1.358	1.397
$R(O_1O_2)$	1.522	1.613	1.609	1.447	1.531
$\angle O_1CO_2$	64.41	66.02	66.11	64.36	66.41
$\angle O_1O_2C$	57.80	56.69	56.94	57.82	56.79
$\angle O_2O_1C$	57.80	56.99	56.94	57.82	56.79

Carbonyl Oxide (**2**)

	HF/3-21G	MP2/3-21G	QCISD/3-21G	HF/6-31G*	MP2/6-31G*
$R(CO_1)$	2.375	2.324	2.338	2.262	2.248
$R(CO_2)$	1.218	1.293	1.329	1.200	1.296
$R(O_1O_2)$	1.633	1.457	1.458	1.482	1.295
$\angle O_1CO_2$	39.62	34.57	34.74	36.60	29.82
$\angle O_1O_2C$	111.99	115.18	113.95	114.53	120.32
$\angle O_2O_1C$	28.39	30.24	31.30	28.87	29.86

TS-2

	HF/3-21G	MP2/3-21G	HF/6-31G*	MP2/6-31G*	MR-CI[2c]
$R(CO_1)$	2.165	2.022	2.123	1.960	1.951
$R(CO_2)$	1.233	1.307	1.208	1.277	1.310
$R(O_1O_2)$	1.821	1.579	1.782	1.452	1.524
$\angle O_1CO_2$	57.23	51.32	57.03	47.77	51.2
$\angle O_1O_2C$	88.07	88.45	88.29	91.60	86.7
$\angle O_2O_1C$	34.70	40.23	34.68	40.63	42.1

b. Optimized Geometries of Transition States for Oxygen Atom Transfer from Dioxirane (**TS-3**) and Carbonyl Oxide (**TS-4**) to Ethylene

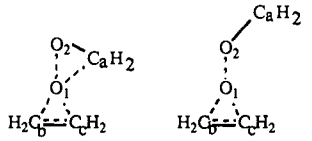

TS-3 **TS-4**

TS-3

	HF/3-21G	MP2/3-21G	CISD/3-21G	QCISD/3-21G	HF/6-31G*	MP2/6-31G*
$R(C_bC_c)$	1.324	1.395	1.363	1.385	1.326	1.384
$R(C_bO_1)$	2.348	1.911	1.995	1.981	2.350	1.904
$R(C_cO_1)$	2.347	1.921	1.995	1.981	2.351	1.904
$R(O_1O_2)$	1.848	1.927	1.894	1.945	1.876	1.885
$R(O_2C_a)$	1.252	1.361	1.311	1.350	1.218	1.328
$R(O_1C_a)$	1.879	1.549	1.641	1.610	1.861	1.445
$\angle C_bC_cO_1$	73.63	68.25	70.03	69.54	73.59	68.68
$\angle C_cC_bO_1$	73.62	69.04	70.03	69.54	73.63	68.68
$\angle C_bO_1C_c$	32.75	42.71	39.95	40.92	32.78	42.64
$\angle O_2O_1C_b$	161.80	156.70	159.72	157.56	162.96	154.49
$\angle O_2O_1C_c$	161.85	157.55	159.72	157.56	161.52	155.51
$\angle O_1O_2C_a$	71.75	52.86	58.26	54.97	70.31	49.84
$\angle O_2C_aO_1$	69.10	82.67	78.92	81.66	71.65	85.54

TS-4

	HF/3-21G	MP2/3-21G	CISD/3-21G	QCISD/3-21G	HF/6-31G*	MP2/6-31G*
$R(C_bC_c)$	1.322	1.347	1.335	1.353	1.323	1.347
$R(C_bO_1)$	2.362	2.321	2.315	2.261	2.441	2.184
$R(C_cO_1)$	2.362	2.321	2.315	2.261	2.441	2.184
$R(O_1O_2)$	1.812	1.643	1.706	1.682	1.845	1.612
$R(O_2C_a)$	1.213	1.269	1.237	1.264	1.190	1.237
$R(O_1C_a)$	2.492	2.375	2.411	2.416	2.515	2.346
$\angle C_bC_cO_1$	73.75	73.13	73.24	72.58	74.28	72.03
$\angle C_cC_bO_1$	73.75	73.13	73.24	72.58	74.28	72.03
$\angle C_bO_1C_c$	32.50	33.75	33.51	34.83	31.44	35.93
$\angle O_2O_1C_b$	163.58	163.08	163.13	162.50	164.23	162.03
$\angle O_2O_1C_c$	163.58	163.08	163.15	162.50	163.23	162.03
$\angle O_1O_2C_a$	109.37	108.67	109.00	109.33	110.02	110.17
$\angle O_2C_1O_a$	43.30	40.93	91.98	41.08	43.58	40.17

[a] Bond lengths in angstroms; angles in degrees.

Table III. Total Energies (au) for Reactants, Transition States, and Products and Potential Barriers (kcal/mol) for the Reactions between Dioxirane, Carbonyl Oxide, and Ethylene

Part a

	HF/3-21G	MP2/3-21G	QCISD/3-21G	MP4SDTQ/3-21G//HF/3-21G	MP4SDTQ/3-21G//MP2/3-21G	QCISD(T)/3-21G//QCISD/3-21G
			Energies			
			Reactants			
dioxirane	−187.552 08	−187.908 22	−187.920 09	−187.920 28	−187.928 49	−187.927 96
carbonyl oxide	−187.527 48	−187.850 92	−187.885 36	−187.867 81	−187.877 54	−187.892 68
ethylene	−77.600 99	−77.784 52	−77.811 54	−77.808 35	−77.810 11	−77.813 98
			Transition States			
TS-2	−187.503 03	−187.822 29		−187.832 50	−187.851 93	
TS-3	−265.114 31	−265.658 98	−265.696 39	−265.673 63	−265.710 61	−265.714 35
TS-4	−265.127 59	−265.633 22	−265.682 67	−265.674 51	−265.684 39	−265.692 24
			Products			
formaldehyde	−113.221 82					
epoxide	−152.000 70					
			Potential Barriers			
$\Delta E_2^{\ddagger}$	30.78	53.92		55.08	48.04	
$\Delta E_{-2}^{\ddagger}$	15.34	17.97		22.16	16.07	
$\Delta E_3^{\ddagger}$	24.32	21.18	22.11	34.51	17.56	17.31
$\Delta E_4^{\ddagger}$	0.55	1.39	8.93	1.04	2.05	9.05

Part b

	HF/6-31G*	MP2/6-31G*	RQCISD/6-31G*//MP2/6-31G*	RQCISD(T)/6-31G*//MP2/6-31G*	MP4SDTQ/6-31G*//HF/6-31G*	MP4SDTQ/6-31G*//MP2/6-31G*
			Energies			
			Reactants			
dioxirane	−188.605 61	−189.107 82	−189.111 70	−189.128 09	−189.123 04	−189.129 67
carbonyl oxide	−188.558 95	−189.052 80	−189.066 94	−189.082 55	−189.067 85	−189.083 08
ethylene	−78.031 72	−78.294 29	−78.313 32	−78.322 15	−78.318 70	−78.319 80
			Transition States			
TS-2	−188.531 93	−189.012 92	−189.039 59	−189.052 09	−189.021 09	−189.045 20
TS-3	−266.572 09	−267.376 36	−267.388 38	−267.422 26	−267.372 64	−267.427 65
TS-4	−266.582 33	−267.323 57	−267.357 91	−267.384 83	−267.366 42	−267.380 66
			Products			
formaldehyde	−113.866 33	−114.167 75	−114.182 48	−114.191 11	−114.189 05	
epoxide	−152.867 35	−153.315 69	−153.328 46	−153.341 37	−153.338 89	−153.341 44
			Potential Barriers			
$\Delta E_2^{\ddagger}$	46.23	59.55	45.25	47.69	63.97	53.01
$\Delta E_{-2}^{\ddagger}$	16.96	25.03	17.16	19.11	29.34	23.77
$\Delta E_3^{\ddagger}$	40.93	16.16	22.99	17.56	43.36	13.69
$\Delta E_4^{\ddagger}$	5.23	14.76	14.02	12.47	12.63	13.94

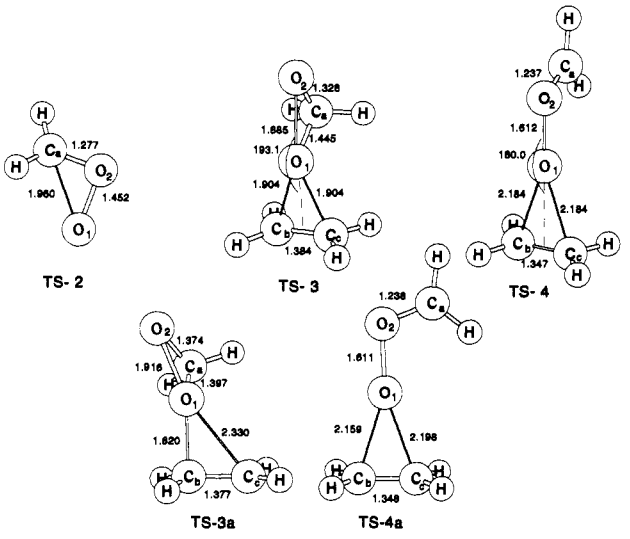

Figure 4. Transition-state geometries at the MP2/6-31G* level for the dioxirane–carbonyl oxide rearrangement (**TS-2**) and for oxygen transfer from dioxirane (**TS-3**) and carbonyl oxide (**TS-4**) to ethylene (constrained to be spiro with identical C–O bond distances) and the corresponding fully optimized transition states (**TS-3a**) and (**TS-4a**).

The potential barrier for ring opening of dioxirane (**1**) to carbonyl oxide (**2**) is prohibitively high, 47.7 kcal/mol (Figure 2). The geometry of the transition structure (**TS-2**) (Figure 4) for this highly endothermic process is consistent with the Hammond postulate and more closely resembles **2** than **1** with the exception of the O–O bond length (1.452 Å), which has only shortened 0.08 Å at the TS (Table IIa). The energy requirements for ring closure of **2** to **1** are also sufficiently high (19.1 kcal/mol) that one should not anticipate a facile equilibration between these two oxidants at room temperature in the absence of vibrational excitation, since other lower activation pathways would surely intervene. Barriers of 54.1 and 22.8 kcal/mol for the interconversions of **1** and **2** have also been reported by Cremer (MP4SDQ/6-31G*).[2a]

Potential Energy Surfaces for Oxygen Atom Transfer. The transition states for dioxirane + ethylene, **TS-3**, and carbonyl oxide + ethylene, **TS-4**, were optimized at six different levels of theory to assess the sensitivity of the geometries of these structures to the calculational level. Initially, the approach of the oxygen to ethylene was constrained to be symmetric, affording identical C–O_1 bond distances. The HF/3-21G and HF/6-31G* calculations give very poor estimates of the O–C_a bond lengths in **TS-3** and the O–O bond length in **TS-4**. Optimization of the geometries at the QCISD/3-21G level and comparison with the MP2/3-21G structures (Table IIb), suggest that the effects of higher excitations

on the TS geometries are not significant. Hence, the geometrically constrained transition structures were optimized at the MP2/6-31G* level (Figure 4).

At first glance the strained but normal covalent structure **1** presents itself as a less nucleophilic reagent than the dioxygen ylide **2**. However, at the MP4SDTQ/6-31G*//MP2/6-31G* level of theory and in the absence of solvent, the activation barriers for oxygen transfer from **1** and **2** to ethylene are indistinguishable at 13.7 and 13.9 kcal/mol, respectively. The roots of the RHF/UHF stability analysis for symmetrical structures **TS-3** and **TS-4** were −0.09 and −0.02, indicating the potential for partial biradical character. Release of the RHF constraint afforded a UHF-stable wave function for **TS-4** with an energy decrease of only 0.73 kcal/mol; however, the UHF calculation on **TS-3** was slow to converge. We had anticipated difficulty with **TS-3**, since extensive CI calculations were found to be essential to getting correct relative energies of dioxirane and its corresponding bis(oxy)methylene biradical.[2d,3a] In addition, much of the experimental community[4a,b] has openly embraced the possibility that dioxiranes can cede an oxygen by a biradical pathway because the open biradical form of dioxirane, dioxymethane, is computed to be only 11.1 kcal/mol[2g] above its ground state (the symmetry and state function correlation arguments pertaining to the three principal biradical configurations of this bis(oxy)methylene biradical had not yet been discussed in the literature). Therefore, we computed energy differences using the QCISD(T) method,[7d] which is known to be satisfactory for partially broken bonds and biradicaloid species.[2k] As noted above, energy differences of 11.6 and 38.0 kcal/mol (QCISD(T)/6-31G*//MP2/6-31G*) between ground-state cyclic **1** and its lowest energy open biradical form **5a** (2π singlet) and the related biradical **5c** (4π singlet), respectively, would tend to exclude a biradical pathway for oxygen atom transfer from **1**. Significantly, the QCISD(T)/6-31G*//MP2/6-31G* barrier for oxygen transfer from **2** is 5 kcal/mol lower than the barrier for epoxidation by **1** (Figure 2), and the origin of the difference can be traced to an overestimation of the triples contribution at the MP4 level (Table IIIb). Since barriers based upon the QCI calculations ought to be more reliable, we suggest that dioxygen ylide **2** is a more efficient oxygen donor than dioxirane, at least in the gas phase. Despite the appearance of nucleophilicity, oxene transfer from carbonyl oxide to ethylene exhibits a barrier that is actually 2.6 kcal/mol *lower* in energy than that for epoxidation with peroxyformic acid.[7e] Because of its lower energy, epoxidation with **1** is less exothermic (51.6 kcal/mol) than oxirane formation from carbonyl oxide (80.2 kcal/mol). A potential barrier of 17.6 kcal/mol for a gas-phase model reaction involving the parent dioxirane (**1**) and ethylene is in good accord with an experimentally determined value of E_a = 14.1 kcal/mol (log A = 7.41) for the epoxidation of ethyl cinnamate with dimethyldioxirane.[3b] Both spiro transition structures **TS-3** and **TS-4** (Figure 4) are consistent with an S_N2 type displacement along the approximate axis of the O–O bond.

Release of all geometry constraints in the transition states for oxygen transfer from **1** and **2** to ethylene afforded unsymmetrical **TS-3a** and planar **TS-4a** with activation barriers of 13.2 and 14.7 kcal/mol (MP2/6-31G*) and 16.7 and 11.9 kcal/mol (QCISD(T)/6-31G*//MP2/6-31G*), respectively. As noted above, the barrier for epoxidation by carbonyl oxide is 4.8 kcal/mol lower than that for oxygen transfer from dioxirane. Transition structure geometries give little indication about the relative position of the TS along the reaction coordinate. The alkene fragment has not been significantly perturbed in either TS, while a major geometric distortion is evident in the oxidizing agent. The much shorter C_b–O bond in **TS-3a** at the MP2 level is worthy of note as is the shorter O–O bond in planar **TS-4a**. Oxygen transfer from **1** is attended by the exothermic formation of a carbon–oxygen double bond and the relief of ring strain (24.7 kcal/mol);[2a] however, both C–O and O–O bond breaking are involved. Epoxidation with the thermodynamically less stable **2** requires breaking a shorter, stronger O–O bond. The O–O bond energy in **1** has been estimated at 36 kcal/mol,[2a] while that BDE in **2** is approximately 61 kcal/mol.[11]

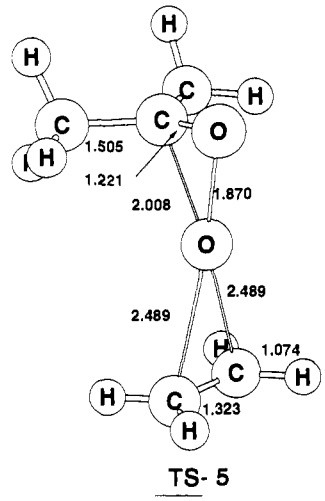

TS- 5

Figure 5. Optimized (HF/6-31G*) transition state for oxygen atom transfer from dimethyldioxirane to ethylene. Distances are in angstroms. Energy: −344.669 63 au.

Significantly, the "electrophilic" oxygen atom in **TS-4a** is essentially a singlet oxygen atom suspended between two fragments each with a nearly completely formed carbon–carbon or carbon–oxygen double bond. Therefore, one should not expect an energy preference for a spiro or a planar orientation of attack on the double bond. The oxygen lone pairs on the central oxygen are almost degenerate at the TS, and the electron density around an oxenoid oxygen is rather spherical in nature. The energy difference between spiro **TS-4** and fully optimized planar **TS-4a** is only 0.53 kcal/mol. A similar observation was noted by Cremer,[2j] who reported a barrier for **TS-4** of 4.7 kcal/mol (HF/6-31G*). In the related oxygen atom transfer from an oxaziridine, both spiro and planar orientations of approach to ethylene were first-order saddle points of almost identical energies.[7f,g] In both cases we suggest that the geometry of the TS will be a reflection of steric interactions and that a special electronic effect is not involved. The more polar carbonyl oxide has a calculated dipole moment of 5.4 D, while that in dioxirane is 3.1 D, which should be reflected in a difference in ground-state solvation. Consistent with this observation, the stabilization energy for hydrogen-bonding a molecule of water to **1** and **2** is 7.0 and 14.3 kcal/mol, respectively (MP4SDTQ/6-31G*//HF/6-31G*). This is consistent with the suggestion of Karlström and Roos[2e] and may provide one explanation for the discrepancy between theoretical and experimental data.

Epoxidation with Dimethyldioxirane. The above theoretical analysis has been conducted on the parent substrates **1** and **2** because of the practical limitations attending calculations at this level of theory on substituted oxidants. However, most of the experimental data involve reactions of dimethyldioxirane[3] and its trifluoromethyl derivative (mellodioxirane)[4c] with substituted nucleophiles. Difluorodioxirane has also been generated in the gas phase, and a facile stereospecifc oxygen transfer to alkenes has been reported.[2l] Ab initio calculations have also suggested that this difluoro derivative is more stable than the parent dioxirane. Despite the lack of substituents, **TS-3** is quite consistent with a bimolecular attack[4b] of an alkene on the simplest cyclic peroxide. The transition structure for epoxidation of ethylene by dimethyldioxirane (Figure 5) is quite similar to **TS-3**, and the HF/6-31G* barrier of 38.7 kcal/mol is in accord with expectation. The comparable HF/6-31G* barrier for epoxidation by **1** is slightly higher ($\Delta E_3^{\ddagger}$ = 40.9 kcal/mol), and the bond distance between the electrophilic oxygen and ethylene (2.489 Å) in **TS-5** is considerably longer. It is worthy of note that the carbon–oxygen bond distance in **TS-3** is 0.45 Å shorter at the MP2 level than at the Hartree–Fock level. Although the MP2/6-31G* level of

(11) The BDE of the O–O bond was estimated by calculating (MP4SDTQ/6-31G*//MP2/6-31G*) the dissociation of H_2COO into a singlet (^1D) oxygen atom and formaldehyde.

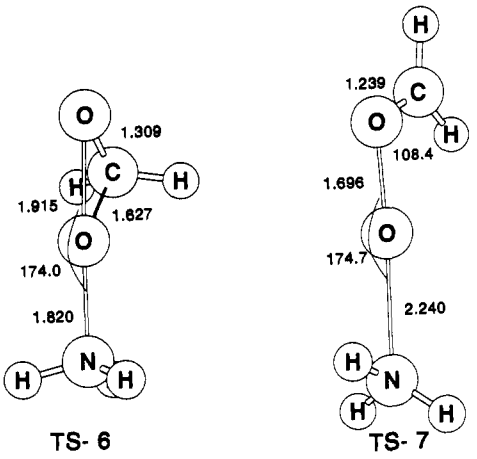

Figure 6. Transition-state geometries (CISD/3-21G) for oxygen atom transfer from dioxirane (**TS-6**) and carbonyl oxide (**TS-7**) to ammonia. Distances are in angstroms, and angles in degrees. Energies: −243.822 12, −243.807 03 au.

theory was not adequate to the task of predicting the geometry of carbonyl oxide itself, it is sufficient for transition structures involving oxygen donation from **2** and for ground-state dimethyldioxirane and its oxygen-transfer reactions. The spiro orientation of this transition structure (Figure 5) possibly reflects both a modest two-electron stabilization due to an interaction of an oxygen lone pair with the π^* orbital of the alkene and the experimentally established sensitivity of this oxygen-transfer reaction to alkene steric effects.[4b] Moreover, it appears that the potential energy surface for the approach of the "electrophilic" oxygen atom from a variety of oxidizing agents to a carbon–carbon double bond is very flat and an unsymmetrical approach directly over one of the carbon atoms does not differ significantly in energy. For example, we have recently found an unsymmetrical TS for the epoxidation of ethylene with peroxyformic acid to be 0.23 kcal/mol lower in energy than the symmetrical spiro orientation.[7e]

Open-Shell Character in Transition States. There has been much speculation in the literature regarding the biradical character of dioxirane in transition structures. The complete active-space multiconfiguration SCF (CASSCF) method provides one of the simplest schemes for looking at the open-shell nature of a subset of orbitals and hence provides a useful tool which is capable of addressing the question of biradical character. CASSCF single-point calculations were carried out on CISD/3-21G-optimized geometries to assess qualitatively whether there was any significant electron transfer between orbitals. In choosing the orbital subspace to include in the CASSCF treatment, we used Pulay's UHF natural orbital (UNO) procedure.[5e] In the case of ethylene and dioxirane, the CASSCF active space consisted of the bonding and antibonding orbitals corresponding to the C–O and O–O bonds in dioxirane, both of which must break as the oxygen atom is transferred (**TS-3**). The CASSCF natural orbital occupation numbers for the C–O bonding/antibonding orbitals are 1.95/0.05, indicating that this bond is still relatively unaffected at this point along the reaction path. The O–O bonding/antibonding orbitals showed occupancies of 1.78/0.22. Hence, the O–O bond is significantly more perturbed than the C–O bond, but the occupation of the antibonding O–O orbital is not sufficient to indicate that at this transition-state geometry the dioxirane moiety is an open-shell biradical. Rather, this result indicates that the O–O bond, although elongated, is still a doubly occupied σ bond. Comparison with the O–O bond in isolated dioxirane shows that in the transition state there is only a 23% elongation, which is again in accord with the observation above. A similar picture emerges for the reaction of ammonia with dioxirane (Figure 6). The CASSCF space is equivalent (i.e. C–O and O–O bonding and antibonding orbitals of dioxirane). The C–O orbital occupancies are identical, while the O–O bonding/antibonding orbital occupancies are slightly modified to 1.80/0.20. For both ethylene and ammonia, the orbitals to which oxygen is transferred (i.e. the ethylene π orbital and the nitrogen lone pair in ammonia) are located in the doubly occupied core. This implies that these transition structures are "early" with respect to oxygen transfer and that the barriers may be attributed largely to the geometric distortion of the dioxirane moiety.

The reaction between ethylene and carbonyl oxide, **TS-4**, exhibits behavior substantially different from that of dioxirane. Similar to **TS-3**, the transition state has an RHF → UHF instability, but with the 6-31G* basis, the root is quite small (−0.02) and the lower solution differs by less than 1 kcal/mol. In order to check the nature of the wave function, a CASSCF/3-21G calculation was performed for the carbonyl oxide and ethylene system starting from RHF orbitals. The active space was chosen to include the three "allylic" π orbitals and the two in-plane oxygen lone pairs of H_2COO as well as the π and π^* orbitals of ethylene. This yielded a CASSCF space of 8 electrons in 7 orbitals consisting of 490 configuration state functions. At convergence, the largest occupancy of an antibonding orbital lying in the COO plane was found to be 0.09, corresponding to the π^* orbital of ethylene. The C–O antibonding orbital of carbonyl oxide lying perpendicular to the C–O π bond also showed an occupancy of 0.09. However, *there is no evidence of any significant biradical character in any of the transition states discussed.* From the orbital occupancies and the transition-state geometries, it is clear that the dioxirane transition state is more advanced in transferring the oxygen atom relative to carbonyl oxide. This is also borne out by the fact that the bond between the migrating oxygen and the ethylene carbons is ~0.3 Å shorter in the dioxirane transition state than in the carbonyl oxide transition state. The relative gas-phase nucleophilicity of the substrate must also be taken into consideration, since the oxygen–nucleophile bond lengths, noted in Figure 6 for the oxidation of ammonia, are even longer (0.42 Å).

Chemical Reactivity of Peroxides. As the complexity of chemical reagents increases, the classic division between electrophilic and nucleophilic species is becoming even more obscure. This is particularly germane to electron-rich oxidizing agents. Typical peroxide bonds, with four oxygen lone pairs of electrons, are deficient in bonding MO's, and the highest occupied MO's (HOMO's) in such compounds are occupied π^* orbitals. In the past, such reagents have been designated as "supernucleophiles", since adjacent pairs of electrons induce an orbital splitting that in principle increases the energy of the HOMO. However, this conventional wisdom has recently been thwarted by gas-phase experiments with HOO^-, where no such enhanced reactivity could be detected.[12] Thus, the "α-effect" nucleophilicity of such species in solution must be ascribed to a solvent effect.

In a cleverly designed mechanistic probe involving thianthrene 5-oxide, which possesses a nucleophilic sulfide moiety and an electrophilic sulfoxide, Adam[4a,c] has provided an internally consistent data base for the comparison of the nucleophilic nature of oxygen atom transfer. In his assignment of nucleophilic character (X_{nu}) in reactions with thianthrene 5-oxide, Adam[4a] assigned an X_{nu} of 1.00 to hydroperoxy anion and a value of X_{nu} = 0.06 to H_2O_2 in the presence of strong acid. These data are in excellent accord with our gas-phase results, where H_2O_2 is essentially unreactive ($\Delta E^{\ddagger}$ = 56 kcal/mol) in the absence of solvent participation or a proton relay, while fully protonated H_2O_2 transfers an oxygen without an activation barrier.[7c] However, the gas-phase epoxidation of ethylene by LiOOH exhibits a calculated (MP4SDTQ/6-31G*//MP2/6-31G*) barrier (12.6 kcal/mol) that is 3.9 kcal/mol *lower* than that for epoxidation by the paradigm electrophile, peroxyformic acid.[7e] A substituted carbonyl oxide was found to be appreciably more nucleophilic in solution than *m*-chloroperbenzoic acid,[4c] but we found barriers of 12.5 kcal/mol for carbonyl oxide and 16.5 kcal/mol for peroxyformic acid in the epoxidation of ethylene. The nucleophile can also exert its influence upon the barrier, since oxygen transfer from LiOOH to ammonia has a higher barrier (20.9 kcal/mol) than that for

(12) (a) Depuy, C. H.; Della, E. W.; Filley, J.; Grabowski, J. J.; Bierbaum, V. M. *J. Am. Chem. Soc.* **1983**, *105*, 2481 and references therein. (b) Klopman, G.; Grierson, M. R. *Croat. Chem. Acta* **1985**, *57*, 1411.

ethylene, although the former is considered to be a better nucleophile. This point is dramatically reinforced by the observation that gas-phase oxygen atom transfer from dioxirane to the simplest sulfoxide (H_2SO) affording its sulfone has a much *lower* barrier (9.6 kcal/mol) than oxidation of H_2S (23.7 kcal/mol) to H_2SO,[13] in good accord with the experiment.[4c] However, the opposite reactivity trend was observed by Murray[3b] in a separate experimental study where the major product of oxidation of a series of aryl methyl sulfides was the sulfoxide. Further oxidation to the sulfone was not observed. In the present study our data are consistent with the fact that dioxirane is more nucleophilic toward ethylene ($\Delta E^{\ddagger}$ = 17.6 kcal/mol) than carbonyl oxide (12.5 kcal/mol), but the opposite situation exists in solution, where carbonyl oxide exhibits a greater "nucleophilicity".[3a,4a] Part of the reactivity of dioxirane has been thought to be due to relief of ring strain. However, the relative potential barriers for oxygen atom transfer from dioxirane (13.7 kcal/mol) and oxaziridine (37.0 kcal/mol) to ethylene suggest that the bond energies are also important. Consistent with this suggestion, oxidations of ammonia by water oxide (H_2OO) and ammonia oxide (NH_3O) exhibit barriers of 1.7 and 31.5 kcal/mol, respectively.[7c] From this litany of conflicting trends, it is obvious that one cannot use a relative rate or an activation barrier as a measure of nucleophilicity without including solvent effects or aggregation of the reactants in solution.

Conclusion

From these data, we conclude that optimization at the MP2 level of theory with MP4 correlation correction appears adequate for oxygen transfer from dioxygen ylides such as water oxide[7a-c] and carbonyl oxide but that QCISD(T) calculations are essential for reliable energetics with the highly strained dioxirane. We add as a cautionary note that transition structures for oxygen atom transfer calculated at Hartree–Fock (**TS-3** and **TS-4**) can be quite misleading, since the first-order saddle points obtained at the MP2 level (**TS-3a** and **TS-4a**) exhibit markedly different geometries (Figure 4). The barrier heights show a remarkable sensitivity to the level of theory with deviations up to 20 kcal/mol. Since oxygen donation from dioxirane exhibits the higher barrier despite its weaker O–O bond and inherent ring strain, we must look elsewhere for the origin of the difference in reactivity. Although the less stable carbonyl oxide form exhibits the greater reactivity as one might anticipate, the intrinsic gas-phase reactivities of these two isomeric oxygen donors are opposite to those observed in solution.[4a] The relative reactivity of dioxirane and carbonyl oxide, as well as that of sulfides and sulfoxides, appears to be dominated to a large extent by solvent and aggregation phenomena. In a number of instances, the intrinsic gas-phase reactivities of these sets of compounds are the opposite of those observed in condensed-phase media. It has been noted that the presence of water increases the rate of epoxidation of alkenes with dimethyldioxirane,[4b] while an increase in solvent polarity has the opposite effect.[1a] In addition to steric interactions, solvent effects must play a major role. Finally, it appears that much of the concern about the involvement of biradical species in these oxygen-transfer reactions appears to have been ill-founded and that predictions based upon calculations of model functional groups void of substituents need not necessarily extrapolate to transition structures involving actual laboratory situations where the electronic structure may be distinctively different.

Acknowledgment. This work was supported in part by grants from the National Science Foundation (CHE-90-20398), the National Institutes of Health (CA 47348-02), and the Ford Motor Co. We are very thankful to the Pittsburgh Supercomputing Center, CRAY Research, the Ford Motor Co., and the C&IT Computing Center at Wayne State University for generous amounts of computing time. J.L.A gratefully acknowledges a fellowship from the CIRIT of the Generalitat Catalunya (Catalonia, Spain), which has made his stay at Wayne State University possible.

(13) McDouall, J. J. W. Unpublished results at the MP4SDTQ/6-31G*//MP2/6-31G* level of theory.